nature geoscience

SUPPLEMENTARY INFORMATION

DOI: 10.1038/NGEO2421

High rates of organic carbon burial in fjord sediments globally

Richard W. Smith, Thomas S. Bianchi, Mead Allison, Candida Savage and Valier Galy

Supplementary Methods

Terrestrial Biomarker Analysis

Freeze-dried sediment containing 3 to 5 mg OC were analyzed for lignin monomers and dimers, and cutin hydroxy acids using the CuO method of Hedges and Ertel (1982)[31]. Briefly, sediments were transferred to stainless steel reaction vials and digested with 330 mg (+/- 4 mg) CuO in 2N NaOH under N_2 at 150 ^{o}C for 3 h. Reaction products were extracted with three successive 3 ml aliquots of peroxide free diethyl ether, evaporated under a stream of N_2, reconstituted in pyridine and converted to trimethylsilyl derivatives using bis-(trimethylsilyl) trifluoroacetamide (BSTFA) at 70^{o}C for 1 hour. Oxidation products were analyzed using an Agilent 6890N gas chromatography instrument coupled to an Agilent 5973N mass spectrometry instrument (GC-MS). The identification of classic lignin-phenols monomers (V, S, and C), as well as 3,5-Bd, was made by comparison with pure standards. Cutin hydroxy acids, lignin dimers and monomers, and benzene carboxylic acids (BCAs) were identified based on published relative retention times and mass spectra. Compound abundances were calculated by normalizing to organic carbon (OC) (mg 100 mg OC^{-1}: Λ). Quantification and % recovery of oxidation products was based on an ethyl vanillin (EVAL) internal standard. The relative response factors (RRFs) to classic lignin-phenol monomers were calculated using the pure compounds in the mixed standard (VAL, VON, VAD, SAL, SON, SAD, CAD, FAD, PAL, PON, PAD, EVAL, ARS), as well as the RRF of 3,5-Bd, the only BCA a standard was available for. The RRFs of cutin hydroxy acids were assumed to be 1, based the on RRFs of the 12-HSA, 16-HHA, and HDDA standards. The RRFs of lignin dimers and extended monomers are assumed to be 1, consistent with other studies due to a lack of available standards.

Source Separation Techniques

CuO Biomarkers

Over 130 biomarkers were identified in this study via CuO oxidation and GC/MS analyses. Commonly, selected lignin monomers including vanillyl (V), syringyl (S), and cinnamyl (C) phenols containing acid, aldehyde, and ketone function groups are quantified from these chromatograms. While their use is less prolific, large amounts of useful oxidation products have been identified in these chromatograms that contain unique sources and degradation pathways. Among these include lignin-dimers[32], cutin hydroxy acids[33], aromatic oxidation products[34], lipid oxidation products[34], and benzene carboxylic acids[35]. Due to the vast diversity of individual biomarkers and source and degradation proxies based on them, we only utilize the total yields of each individual biomarker class (i.e. lignin-dimers), and only mention the specific function of proxies that are telling of sedimentary composition. Briefly, lignin-dimers relate structural information of the lignin macromolecule and contain additional source and degradation information, cutin products are sourced from plant soft-tissue exclusively and are unique to monocots vs. dicots, benzene

carboxylic acids are formed in both plants and soils, and aromatic and lipid oxidation products are produced from both terrestrial and marine material (although based on regressions vs. $\delta^{13}C$ in this study, they are found to be predominantly terrestrial). Downcore variations in lignin-phenol concentration are shown along with bulk % OC in Figure S4, and show little indication of post-depositional degradation .

Sediment OC Composition

Source identification was aided by the collection of a large suite of terrestrial end-members, including soils, and soft and woody tissue from angiosperm and gymnosperm plants common in the region. In this study we successfully separated sediment OC composition into five distinct sources; OC_{marine}, and OC_{terr} in the form of angiosperm soft plant tissue (OC_a), angiosperm woody plant tissue (OC_A), soils (OC_{soil}), and fossil carbon from weathered sedimentary bedrock (OC_{fossil}) (Figure S5). Due to large variations in composition downcore, we calculated these values as the "average" of all 2 cm sediment samples in each core (Table S1). In this way we minimize yearly/decadal variability and observe a signal that is integrated temporally on a timescale of the last few hundred years.

OC_{fossil} contributions were determined to be constant throughout the spatial and temporal limits of the study using the regression method of Galy et al. (2008)[36], which produced a linear trend (Figure S3). Therefore this source could be quantitatively separated. Results from this technique suggest OC_{fossil} is a constant 0.33% of total sediment mass in all selected sediment samples from each core, which we assume is representative of the entire length of the cores. We therefore use the following equation

$$f_{fossil} = 0.33 \,/\, \%\,OC \qquad (1)$$

where, f_{fossil} is the fraction of OC that is fossil in origin, 0.33 is the slope of the regression in Figure S3, and %OC is the average %OC value for each core. We then applied a three end-member mixing model to the remaining OC to separate OC_{marine}, OC_{soil}, and $OC_{plant.}$ $\delta^{13}C$ and 3,5:V values were used as metrics in the mixing model, as they varied to a much wider extent between sources, than in separate samples from any one source, providing source-specific OM signatures and making quantitative reconstruction possible. 3,5- dihydroxybenzoic acid is found exclusively (with minor exceptions) in soils[37], and when calculated relative to V phenols, mixing between fresh plant material and soils can be observed. Based on collection of terrestrial material in Fiordland, $\delta^{13}C$ values are the most depleted in OC_{plant} (-29.1‰), slightly enriched in OC_{soil} (–28.4‰), and significantly enriched in OC_{marine} (-18‰) relative to terrestrial fractions. However, due to significant contributions of OC_{fossil}, this fraction must be subtracted from the OC yield used in the three end-member mixing model

$$\delta^{13}C_{modern} = \delta^{13}C_{plant} * f_{plant} + \delta^{13}C_{soil} * f_{soil} + \delta^{13}C_{marine} * f_{marine} \qquad (2)$$

$$3,5{:}V_{measured} = 3,5{:}V_{plant} * f_{plant} + 3,5{:}V_{soil} * f_{soil} + 3,5{:}V_{marine} * f_{marine} \qquad (3)$$

$$f_{plant} + f_{soil} + f_{marine} = 1\text{-}f_{fossil} \quad (4)$$

where, f_{plant}, f_{soil}, and f_{marine} represent the fraction of OM in a sediment sample derived from fresh vascular plants, soil, and marine plankton, $3{,}5{:}V_{measured}$ is the observed sediment value, $\delta^{13}C_{modern}$ is the OC_{fossil} corrected observed sediment value (see below), and $\delta^{13}C_{plant}$ and $3{,}5{:}V_{plant,}$ $\delta^{13}C_{soil}$ and $3{,}5{:}V_{soil,}$ and $\delta^{13}C_{marine}$ and $3{,}5{:}V_{marine}$ are the chosen end-member values of $\delta^{13}C$ and 3,5:V, respectively.

The isotopic signature of OC_{fossil} must be removed from the bulk $\delta^{13}C$ values so the "OC_{fossil} free" $\delta^{13}C$ signature can be applied used as $\delta^{13}C_{measured}$ in equation (2). Based on the average $\delta^{13}C$ of OC_{fossil} in the Southern Alps of -21.1‰[38], we used the following two end-member mixing equations:

$$\delta^{13}C_{measured} = \delta^{13}C_{fossil}*f_{fossil} + \delta^{13}C_{modern}*f_{modern} \quad (5)$$

$$f_{fossil} + f_{modern} = 1 \quad (6)$$

where, $\delta^{13}C_{measured}$ is the observed $\delta^{13}C$ value of the sediment sample, $\delta^{13}C_{fossil}$ is the fossil end-member from the Southern Alps[38], $\delta^{13}C_{modern}$ is the average of OC_{soil} and OC_{plant} end-member $\delta^{13}C$ values, and f_{fossil} and f_{modern} represent the OC fraction composed of fossil (i.e. kerogen and graphite from sedimentary bedrock) and modern (soils and vascular plant material) organic constituents.

Lignin-phenols produced from the oxidation of the lignin macromolecule are indicative of the original lignin source. Particularly, these phenols can be used to differentiate between angiosperm (flowering plants) and gymnosperm lignin, as well as between hard (wood) and soft-tissue (tree leaves, conifer needles, grasses). Syringyl (S) phenols are produced only from the oxidation of angiosperm lignin, and cinnamyl (C) phenols are produced primarily from the oxidation of soft plant tissues, while vanillyl (V) phenols are ubiquitous in vascular plant lignin[39]. Therefore, S/V and C/V ratios provide accurate source separation of lignin, provided that acid to aldehyde functional group ratios of syringyl ([Ad/Al]s) and vanillyl ([Ad/Al]v) phenols are not significantly elevated relative to fresh material, which can indicate selective degradation of S and C phenols[40], or phenol fractionation during sorptive processes[41]. [Ad/Al]s and [Ad/Al]v values of lignin in Fiordland sediments was not observed to be significantly higher than in fresh plant material or soils, and therefore our S/V and C/V ratios can be successfully used to separate plant material into two distinct sources; woody, and non-woody. Additionally, S/V and C/V ratios, as indicated by PCA, are a function of only soft and woody plant contributions in sediments and not the absolute OC_{terr} abundance, and therefore it was possible to separate these pools without affecting the larger 3 end-member mixing model.

The S/V and C/V source plot in Figure S6 includes regional end-members. End-members were chosen to represent gymnosperm soft and hard tissue, angiosperm soft and hard tissue, and also submerged woody material removed from cores, and leaf litter taken at the mouth of a small river. Sediments from all six cores included on this plot are observed to mix between angiosperm soft tissue (leaves), and the submerged wood end-member. Sedimentary plant tissue in general in this study was observed to originate entirely from angiosperms, eliminating

gymnosperm material as a potential end-member. The submerged wood samples (n=3) reflect a similar lignin source signature as angiosperm woody, yet exhibit slightly more reduced S/V values. However, Ad/Al ratios are elevated in the submerged wood, and $\delta^{13}C$ values are slightly more enriched. This evidence suggests that the unidentified submerged woody material is angiosperm wood that has undergone natural diagenetic variation at the bottom of the fjord. As sediment source values seem to reflect mixing towards this end-member rather than fresh material, it is more accurate to use these end-member values rather than fresh angiosperm woody material. Additionally, the vast majority of variation in values can be described purely by S/V ratios, and no gymnosperm material seems to be influencing observed C/V values. Therefore, fractional contributions of angiosperm wood and leaves were determined as follows:

$$S/V_{measured} = S/V_a * f_a + S/V_A * f_A \quad (7)$$

$$f_{a(plant)} + f_{A(plant)} = 1 \quad (8)$$

where, $S/V_{measured}$ is the observed sedimentary ratio of S and V phenol yields, S/V_a and S/V_A are the measured end-member S and V phenol ratio yields of collected terrestrial material, and $f_{a(plant)}$ and $f_{a(plant)}$ are the determined fractional contributions of angiosperm leaves and woody to total plant material, respectively, in sediments. The OC_{plant} end-member values used in equations (2,3) was determined by multiplying the end-member values of angiosperm leaf and wood ($\delta^{13}C$, 3,5:V) by $f_{a(plant)}$ and $f_{A(plant)}$, respectively.

As f_{fossil}, f_A, f_a, f_{soil}, and f_{marine} were determined in three different sets of equations (based on biomarker yields exclusive to the source contributions being measured), it is necessary mathematically set them equal to unity, with respect to the way they were initially calculated. f_{fossil}, f_{soil}, f_{marine} and f_{terr} were calculated with respect to each other, and their contributions equal unity. f_A and f_a were calculated as fractional contributions to f_{plant}. Therefore, the values must be corrected as follows:

$$f_A = f_{A\,(plant)} * f_{plant} \quad (9)$$

$$f_a = f_{a\,(plant)} * f_{plant} \quad (10)$$

where, f_A and f_a are the fractional contributions of angiosperm wood and leaves to total sedimentary OC, and the remaining parameters are taken from equations (7,8).

The resulting mass balance equation is:

$$f_a + f_A + f_{soil} + f_{fossil} + f_{marine} = 1 \quad (11)$$

The values, determined for each of the six scores sampled in this study, are represented visually in Figure 3. These fractions are combined with bulk marine and terrestrial fractions determined in Knudson et al. (2011)[42], and averages of each fjord are shown in Table S4.

Burial Rates

Rate Calculation Techniques

Linear sedimentation rates (Figure S2) were converted to MARs with the following equation:

%OC x SR x (porosity – 1) x bulk density

where, SR is the sedimentation rate in cm yr^{-1}, porosity is assumed to be 0.77[10,43] and bulk density is assumed to be 1.85 g cm^{-3}[10,43]. Porosity and bulk density values are taken from average Patagonian values, which are the closest in latitude to NZ fjord of published fjord sedimentary values. Organic carbon accumulation rates (OC ARs) were calculated by multiplying MARs by the weight fraction of OC, which for each core is represented as the average %OC value of all 2 cm sediment fractions. Finally, to estimate the total amount of CO_2 sequestered in Fiordland, OC ARs are converted to g km^{-2} yr^{-1} and multiplied by the total surface area of all 14 fjords, as well as by a correction factor of 0.8 for deep burial preservation efficiency[1].

Potential Bias

The second bias we would like to address is the potential overestimation of burial rates based on the location of sediment cores included in the global dataset. In general, it is common for the primary depositional zones, or fjord basins in this case, to be selected for coring in order to obtain a higher age resolution. Large variations in fjord basin morphology and a lack of data from sill and slope regions prevent a thorough consideration of all depositional zones with 'weighted' OC contributions. There is reason to believe however that this bias is small. One of the few studies fully addressing basin size in Nordasvannet, Norway, concludes that 88% of the entire fjord surface area is represented by basins and the remaining smaller fraction by sills and slopes[44]. Additionally, slopes can contain large volumes of OC_{terr} from landslides[46] that do not fully enter basins[38].

Supplementary Tables

Table S1. Average bulk elemental and biomarker yields and proxies for sediment cores and terrestrial soils and vegetation. Error is represented as one standard deviation. n is the # of sediment samples in each core or vegetation type. CA = Crooked Arm, DC = Deep Cove, MR = Malaspina Reach, LS = Long Sound, SC = Supper Cove, BA = Broughten Arm. "Vegetation End-member" is calculated as the weighted average of submerged (angiosperm) wood and non-woody angiosperm tissue, while "Marine End-member" is obtained from the references given. Biomarker yields are summed for each class and are represented in lambda notation as mg 100 mg OC^{-1} (lignin-monomers: Λ_8, cutin: Λ_{CA}, benzene carboxylic acids: Λ_{BCA}, lignin-dimers: Λ_{DIMERS}).

Sediment Core	n	%OC	$\delta^{13}C$	$\delta^{15}N$	C/N	3,5:V	S/V	C/V	Λ_8	Λ_{CA}	Λ_{BCA}	Λ_{DIMERS}
CA	19	6.3 ± 2.4	-28.1 ± 0.5	1.2 ± 0.9	26.8 ± 7.1	0.046 ± 0.019	1.54 ± 0.24	0.08 ± 0.02	9.0 ± 3.7	2.8 ± 1.6	0.9 ± 0.3	1.4 ± 0.8
DC	21	8.8 ± 1.4	-27.6 ± 0.3	2.0 ± 0.7	24.2 ± 4.7	0.058 ± 0.011	1.29 ± 0.08	0.10 ± 0.03	6.5 ± 1.2	2.7 ± 1.2	1.0 ± 0.3	0.9 ± 0.4
MR	11	3.7 ± 0.2	-24.8 ± 0.2	6.1 ± 0.4	14.7 ± 0.5	0.056 ± 0.008	1.37 ± 0.12	0.07 ± 0.02	4.7 ± 2.2	1.0 ± 0.4	0.9 ± 0.3	0.6 ± 0.2
LS	12	4.0 ± 0.6	-25.9 ± 0.3	4.8 ± 0.8	18.9 ± 0.8	0.069 ± 0.003	1.52 ± 0.10	0.08 ± 0.02	3.4 ± 0.8	1.4 ± 0.3	0.7 ± 0.1	0.5 ± 0.1
SC	4	4.5 ± 2.2	-27.2 ± 0.2	3.0 ± 0.6	21.9 ± 1.4	0.070 ± 0.004	1.38 ± 0.03	0.13 ± 0.02	5.3 ± 1.1	1.6 ± 0.7	1.6 ± 0.6	0.8 ± 0.5
BA	10	5.6 ± 0.6	-26.5 ± 0.1	3.7 ± 0.2	19.6 ± 0.5	0.041 ± 0.008	1.31 ± 0.04	0.05 ± 0.01	6.8 ± 1.0	1.4 ± 0.6	0.9 ± 0.2	0.9 ± 0.4
Terrestrial End-Members												
Leaf litter	1	44.1	-30.2	-0.6	46.4	0.038	1.18	0.06	8.1	3.2	0.8	1.5
Angiosperm Leaf	6	48.2 ± 4.1	-32.7 ± 1.2	-0.1 ± 1.7	50.6 ± 23.5	0.046 ± 0.055	1.13 ± 0.42	0.20 ± 0.17	4.6 ± 3.5	6.6 ± 5.0	0.4 ± 0.3	0.5 ± 0.3
Gymnosperm Needle	1	49.9	-33.8	-4.6	111	0.124	0.21	0.06	3.4	3.9	0.8	0.8
Submerged wood	3	38 ± 6.2	-26.8 ± 0.1	-4.7 ± 4.1	181 ± 149	0.004 ± 0.003	1.51 ± 0.49	0.01 ± 0.01	21.1 ± 5.4	0.0 ± 0.0	0.3 ± 0.1	4.4 ± 2.4
Angiosperm wood	2	47.0 ± 2.2	-30.9 ± 0.9	-1.3 ± 4.6	112 ± 5.3	0.027 ± 0.031	4.07 ± 1.62	0.04 ± 0.05	13.3 ± 5.6	2.1 ± 3.0	0.2 ± 0.3	1.3 ± 0.2
Gymnosperm wood	1	49.6	-29.7	0.0	825	0.002	0.01	0.01	11.0	0.0	0.1	4.4
Soils	8	20.4 ± 22.1	-28.4 ± 1.4	1.8 ± 1.5	21.8 ± 12.2	0.112 ± 0.044	0.61 ± 0.19	0.16 ± 0.08	3.1 ± 1.8	3.8 ± 5.8	1.3 ± 0.7	0.8 ± 0.5
Vegetation End-Member	11	41.9 ± 5.3	-29.1 ± 0.5	-2.9 ± 3.2	131 ± 98.9	0.02 ± 0.02	1.43 ± 0.49	0.08 ± 0.07	14.8 ± 4.7	2.5 ± 1.9	0.3 ± 0.2	2.9 ± 1.6
Marine End-Member		N/D	-18.23 ± 0.05[a]	4.71 ± 0.17[a]	6.63[b]	0	N/A	N/A	0	0	N/A	0

References: a: McLeod and Wing 2009[19], b: Schuller and Savage 2011[45]

Table S2. Compiled sedimentary data for Fiordland, NZ. Areas are obtained from Syvitsky (1987). Sedimentation rates and %OC (w/w) are from cores collected and analyzed in this study and from Knudson et al. (2011) and Pickrill et al., (1993). Measured values (Sed. Rate and %OC) are given here as the mean of individual samples from the # of compiled cores. Error is represented as one standard deviation, and is propagated through subsequent calculations using standard mathematical theory. The average $C_{org}BR$ is used for Fjords with no available sedimentary data, indicated by *. Deep burial efficiency is assumed to be 80%, from Berner (1982) (1).

Fjord	Area	Reference	# Cores	Sed. Rate	%OC	Sed. AR	C_{org} AR	C_{org} BR	CO_2 seq.
	km^2			$cm\ yr^{-1}$		$g\ m^{-2}\ yr^{-1}$	$gC\ m^{-2}\ yr^{-1}$	$gC\ m^{-2}\ yr^{-1}$	$ton\ yr^{-1}$
Milford	25.3	2	1	0.268	2.03	1140	23.2	18.6	1730 ± 111
Bligh Sound	21.1	-	0					12.1*	936 ± 294
George Sound	32.9	2	3	0.087 ± 0.018	0.98	370 ± 76.6	3.63 ± 0.69	2.90 ± 0.55	350 ± 39.9
Caswell Sound	17.5	-	0					12.1*	776 ± 79.7
Charles Sound	15.9	-	0					12.1*	705 ± 72.5
Nancy Sound	13.9	3	2	0.204	3.75	868	32.6	26.1	1330 ± 23.5
Thompson/Bradshaw	49.3	2,3	3	0.113 ± 0.048	2.20	481 ± 204	10.6 ± 4.49	8.48 ± 3.59	1530 ± 263
Doubtful	83.7	1	3	0.079 ± 0.027	6.91 ± 2.54	336 ± 115	23.2 ± 11.7	18.6 ± 9.36	5700 ± 684
Dagg Sound	14.7	-	0					12.1*	652 ± 67.0
Breaksea	61.5	1	1	0.038	5.61 ± 0.63	162	9.07 ± 1.02	7.26 ± 0.82	1640 ± 59.4
Dusky	181	1	1	0.012	4.53 ± 2.17	51.1	2.31 ± 1.11	1.85 ± 0.88	1230 ± 64.9
Chalky	110	-	0					12.1*	4880 ± 502
Long Sound	93	1, 3	3	0.094 ± 0.022	4.00 ± 0.61	400 ± 93.6	16.0 ± 4.47	12.8 ± 3.58	4360 ± 262
Total	720								25800 ± 2520

References: 1, *This study*; 2, *Knudson et al., 2011*[11]; 3, *Pickrill et al., 1993*[10]

Table S3. Organic Carbon (OC) composition of Fiordland sediments. Error is represented as one standard deviation. f_{marine} = fraction of marine (phytoplankton, macroalgae) OC, f_{fossil} = fraction of ancient (kerogen, graphite) OC sourced from sedimentary bedrock, f_{terr} = fraction of all modern terrestrially source OC (including vegetation and soil), f_{soil} = fraction of OC from soils, f_a = fraction of non-woody angiosperm tissue, f_A = fraction of woody angiosperm tissue. f_{fossil} is determined with a ^{14}C vs. %OC regression method[36]. f_{marine}, $f_{soil,}$ and f_{plant} (the fraction of OC derived from non soil-incorporated fresh vascular plant vegetation) were calculated with a three end-member mixing model with $\delta^{13}C$ and 3,5:V as metrics. f_{terr} is the sum of f_{soil} and f_{plant}. f_a and f_A are components of both soil and fresh vegetation, and were calculated using a two end-member mixing model with C/V as a metric.

Fjord	Reference	f_{marine}	f_{fossil}	f_{terr}	f_{soil}	f_a	f_A
Milford	2	0.43		0.57			
Bligh Sound							
George Sound	2	0.45 ± 0.04		0.55 ± 0.04			
Caswell Sound							
Charles Sound							
Nancy Sound							
Thompson/Bradshaw	2			0.5 ± 0.02			
Doubtful	1,2	0.18 ± 0.16	0.03	0.81 ± 0.16	0.40 ± 0.09	0.15 ± 0.09	0.25 ± 0.14
Dagg Sound							
Breaksea	1	0.22	0.03	0.77	0.27	0.10	0.4
Dusky	1	0.14	0.03	0.86	0.57	0.17	0.11
Chalky							
Preservation Inlet							
Long Sound	1	0.25	0.03	0.86	0.58	0.05	0.09

References: 1, *This Study;* 2, *Knudson et al., 2011*[42]

Table S4. Fraction modern measurements of 2 selected samples from each core. Age corrections are based on the depth in the core and ^{210}Pb determined linear sedimentation rates.

Core	MR	MR	CA	CA	DC	DC	LS	LS	SC	SC	BA	BA
Depth (cm)	6-8	16-18	4-6	10-12	2-4	10-12	12-14	6-8	2-4	6-8	2-4	4-6
%OC	3.60	3.45	10.75	8.26	8.60	7.38	3.77	3.42	1.94	6.36	4.51	4.59
Measured Fm	0.88	0.83	0.94	0.83	0.97	0.93	0.85	0.85	0.85	0.87	0.89	0.91
uncertainty	0.004	0.004	0.005	0.0038	0.0042	0.0043	0.0048	0.0036	0.0034	0.0042	0.0039	0.0043
Age corrected Fm	0.89	0.86	0.94	0.84	0.98	0.94	0.87	0.85	0.87	0.93	0.89	0.92

286 **Supplementary Figures and Legends**

287 **Figure S1 –** Fiordland, NZ and coring locations

288

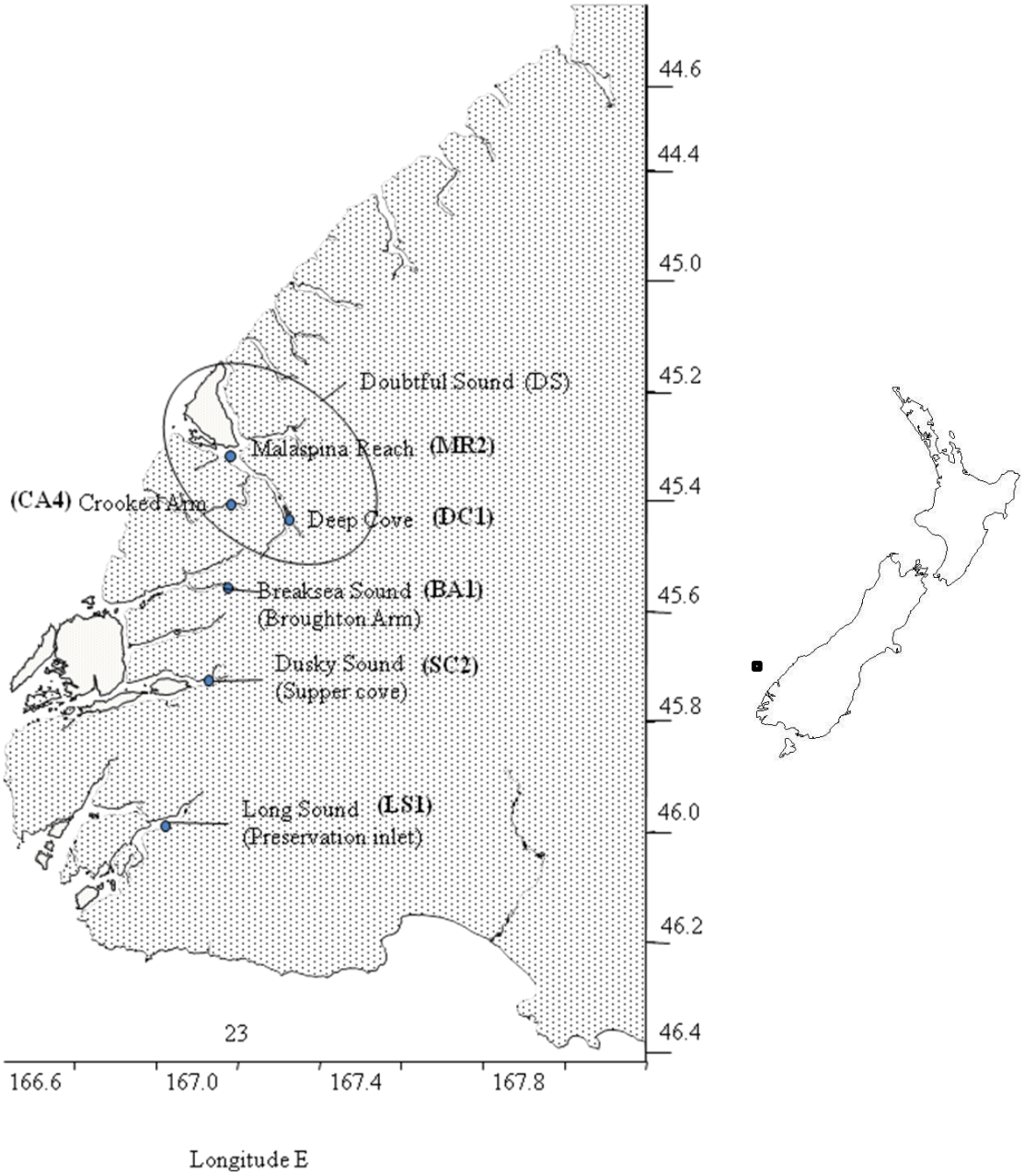

289

290

291

292

293 **Figure S2** – Unsupported ^{210}Pb activities and calculated maximum linear-
294 sedimentation rates (LSR) in six Fiordland cores.

295

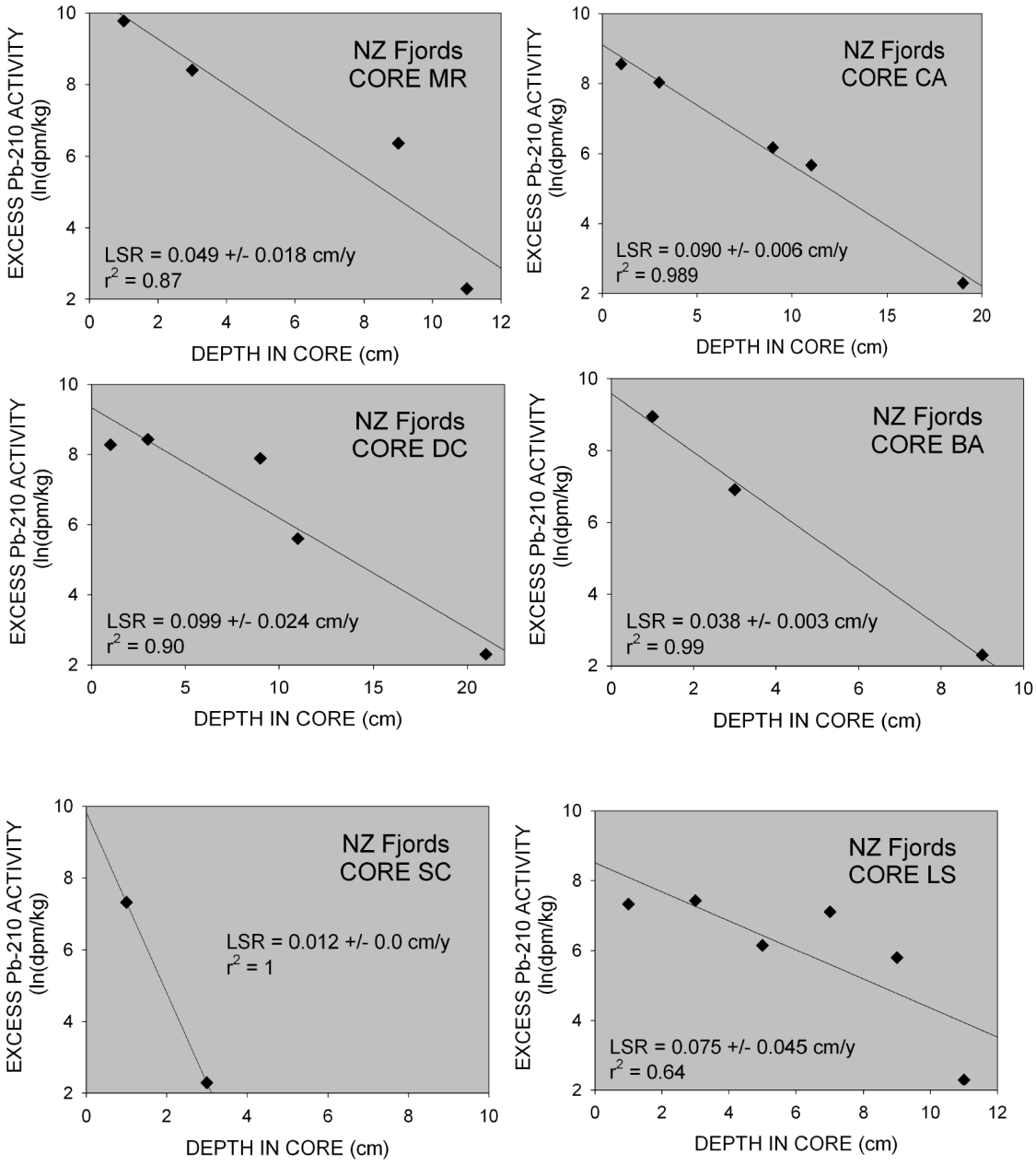

296

297

298

299

300

301

Figure S3 – Regression technique for calculating %Fossil OC and the modern terrestrial fraction modern (fm) end-member, from Galy et al. (2008), as determined by $\Delta^{14}C$ and %OC analyses. The linear trend suggests fossil contributions are static throughout Fiordland sediments.

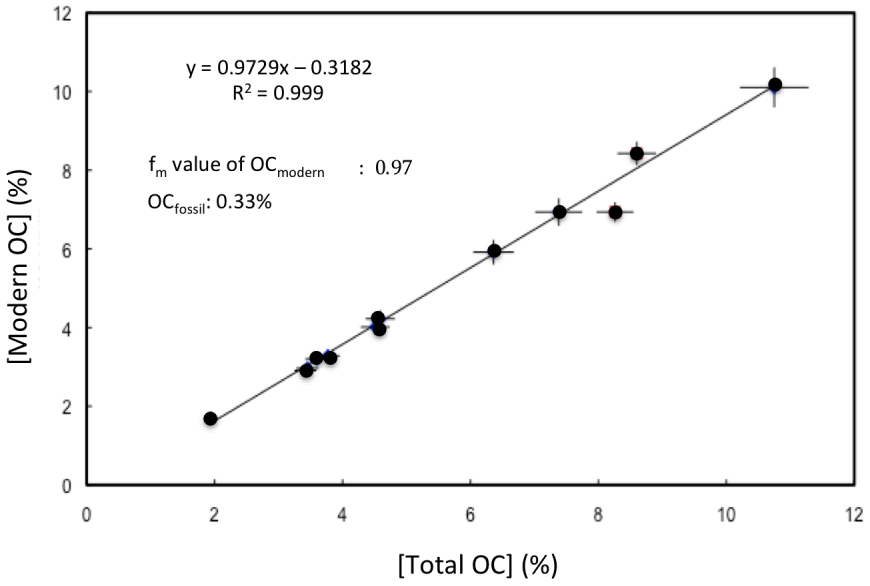

317 **Figure S4 –** Downcore values of %OC (w/w) and lignin concentrations (Λ_8 : mg 8
318 S,V,C phenols 100 mg OC^{-1} in six Fiordland cores.

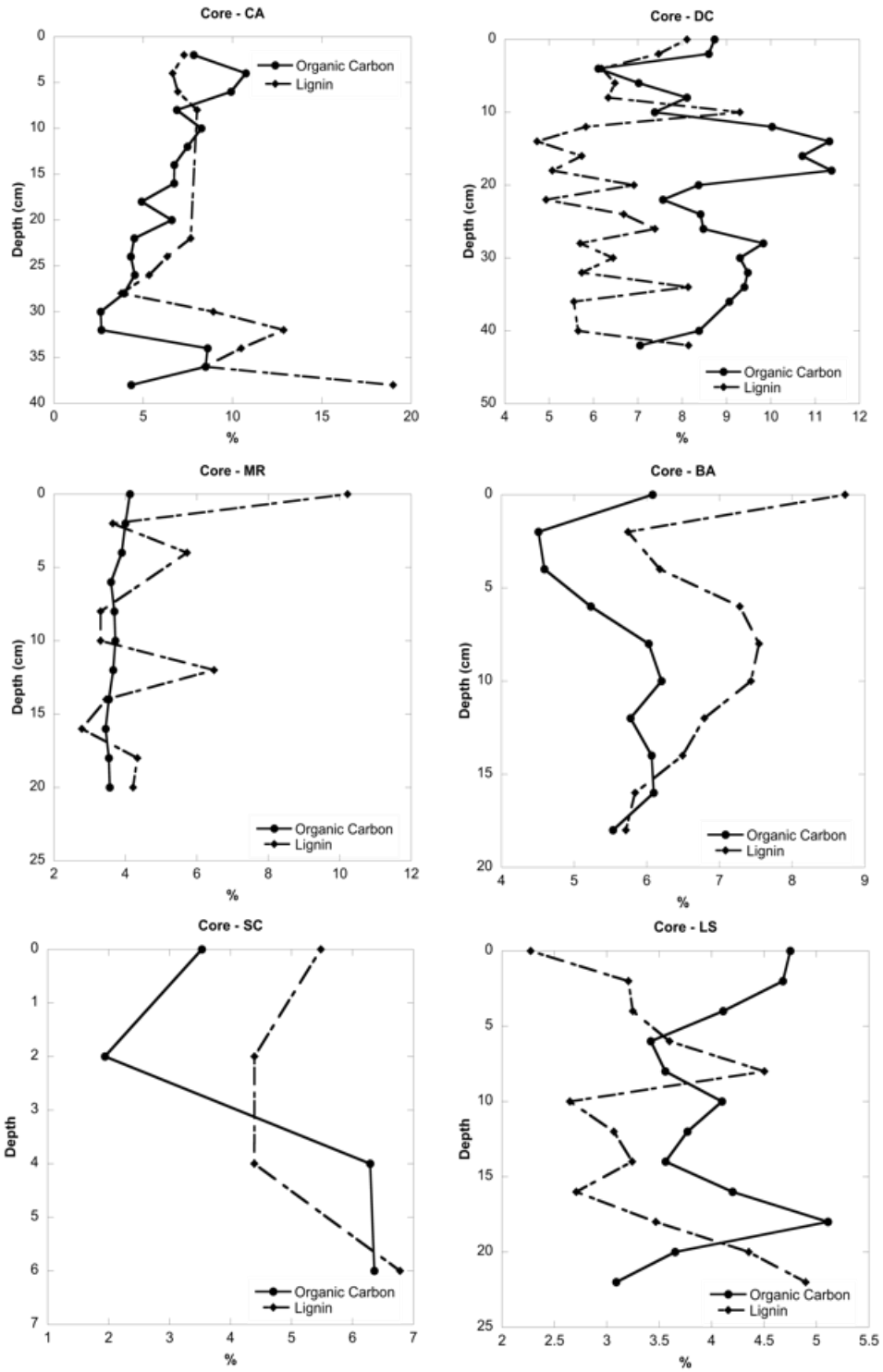

319

320

321

322 **Figure S5** – OC source attribution in sediment cores from Fiordland, NZ collected
323 for this study. a) initial 3 end-member separation. Boxes represent the mean value
324 of each end member, and error bars represent one standard deviation. B) 5 end-
325 member source separation aided by S/V and C/V ratios and $\Delta^{14}C$ analysis.

326

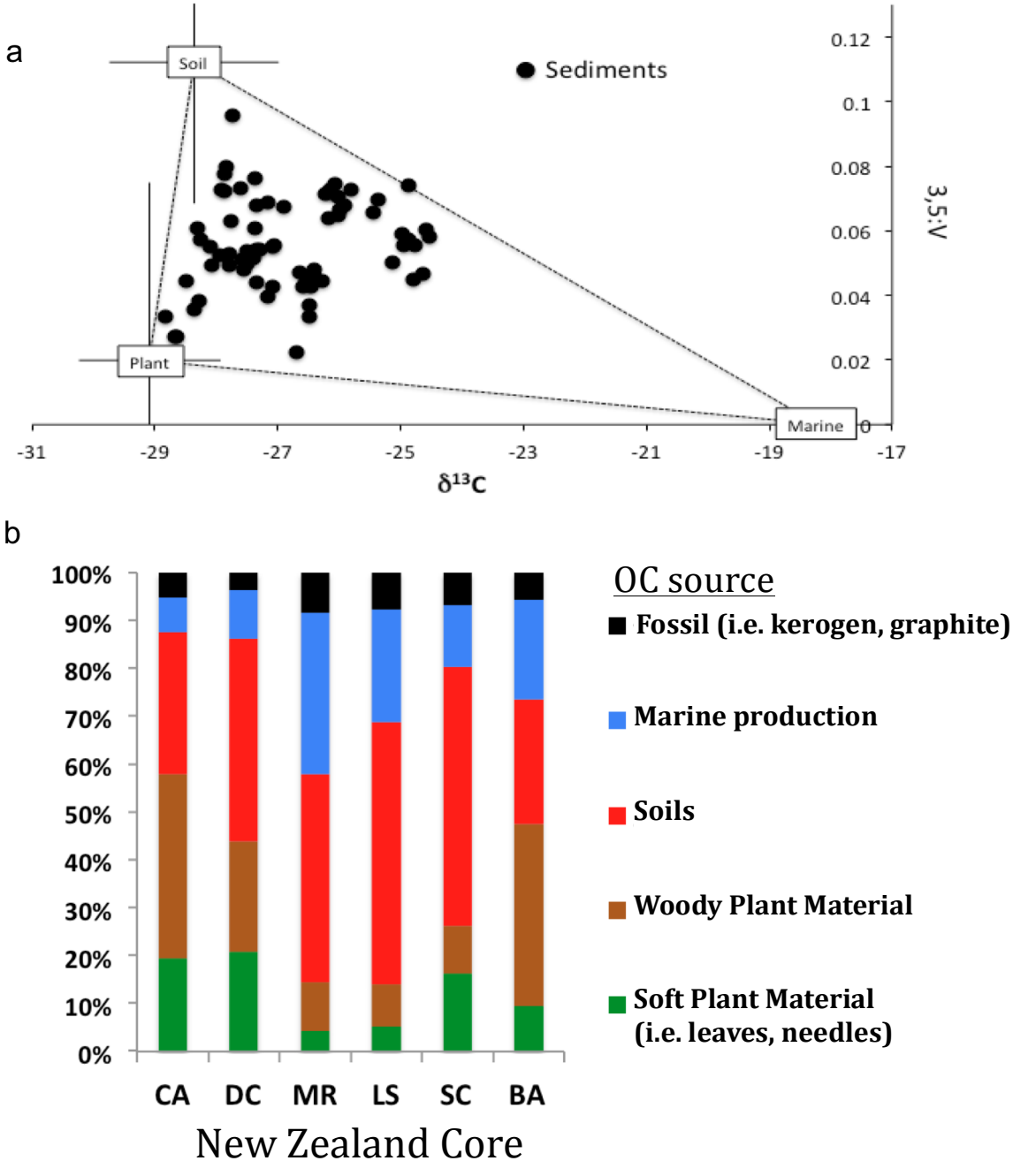

327

328

Figure S6 – Lignin-phenol source plot. Boxes represent average values and one standard deviation of replicate terrestrial end-member measurements collected from the Fiordland watershed. A: angiosperm wood, SW: submerged wood, LL: leaf litter, a: angiosperm leaves, G: gymnosperm woody material, g: gymnosperm needles.

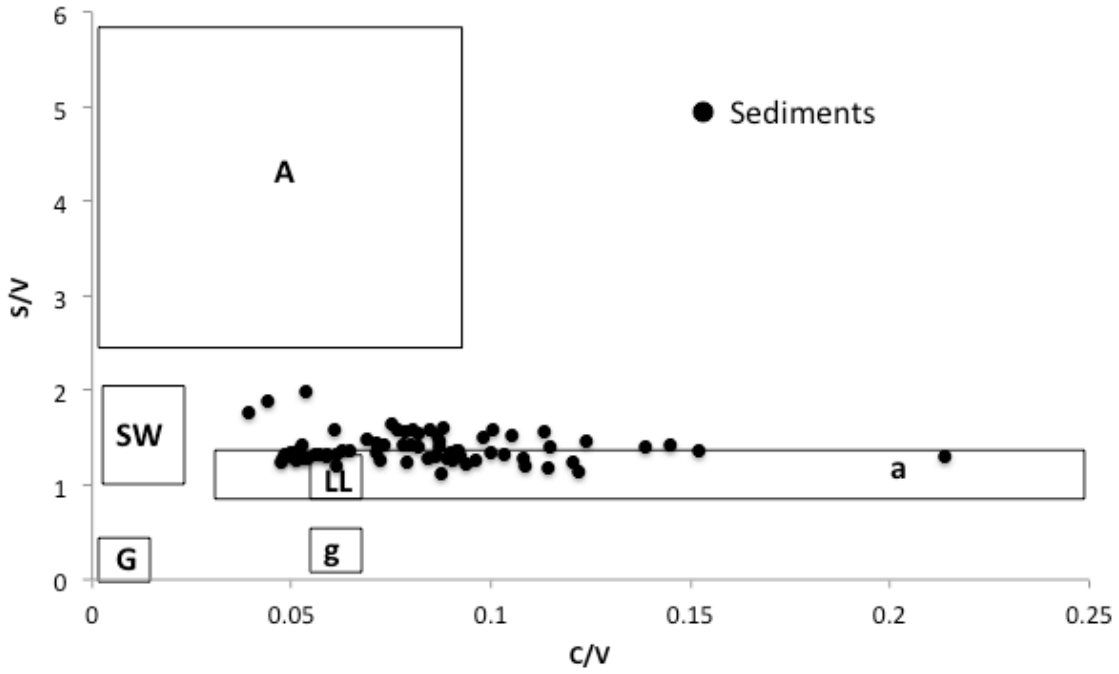

Supplementary References (Including references used in the global fjord dataset but not in the main text)

31. Hedges, J. I. & Ertel, J. R. Characterization of lignin by gas capillary chromatography of cupric oxide oxidation-products. *Anal.Chem*. **54**,174-178 (1982).

32. Goñi, M. A. & Hedges, J. I. Lignin dimers: Structures, distribution, and potential geochemical applications. *Geochim. Et Cosmochim. Acta* **56**, 4025-4043 (1992).

33. Goñi, M. A. & Hedges, J. I. Cutin-derived CuO reaction products from purified cuticles and tree leaves. *Geochim. Et Cosmochim. Acta* **54**, 3065-3072 (1990).

34. Goñi, M. A. & Hedges, J. I. Sources and reactivities of marine-derived organic matter in coastal sediments as determined by alkaline CuO oxidation. *Geochim. Et Cosmochim. Acta* **59**, 2965-2981 (1995).

35. Dickens, A. F., Gudeman, J. A., Gelinas, Y., Baldock, J.A., Tinner, W., Sheng Hu, F. & Hedges, J. I. Sources and distribution of CuO-derived benzene carboxylic acids in soils and sediments. *Org. Geochem.* **38**, 1256-1276 (2007).

36. Galy, V., France-Lanord, C. & Lartiges, B. Loading and fate of particulate organic carbon from the Himalaya to the Ganga-Brahmaputra delta. *Geochim. Et Cosmochim. Acta* **72**, 1767-1787 (2008).

37. Prahl F. G., Ertel J. R., Goni M. A., Sparrow, M. A. & Eversmeyer, B. Terrestrial organic carbon contributions to sediments on the Washington margin. *Geochim. Et Cosmochim. Acta,* **58**, 3035-3048 (1994).

38. Hilton, R. G, Galy, A. & Hovius, N. Riverine particulate organic carbon from a pristine, active mountain belt: the importance of vegetation and landslides. *Glob. Biogeochem. Cycles.* doi:10.1029/2006GB002905 (2008).

39. Sarkanen, K. V. & Ludwig, C. H. *Lignins*. Wiley-Inter-science, 916p (1971).

40. Hedges, J. I., Blanchette, R. A., Weliky, K. & Devol, A. H. Effects of fungal degradation on the CuO oxidation products of lignin: A controlled laboratory study. *Geochim. Et Cosmochim. Acta* **52**, 2717-2726 (1988).

41. Hernes, P. J., Robinson, A. C. & Aufdenkampe, A. K. Fractionation of lignin during leaching and sorption and implications for organic matter "freshness." *Geophys. Res. Lett.* **34**, L17401 (2007).

42. Knudson, K. P., I. L. Hendy, H. L. Neil. Re-examining Southern Hemisphere westerly wind behavior; insights from a late Holocene precipitation reconstruction using New Zealand fjord sediments. *Quat. Sci. Rev.* **30**, 3124-3138.

43. Pantoja, S., Iriarte, J. L., Gutierrez, M. & Calvete, C. The Southern Chile Continental Margin. In: Liu, K. K., Atkinson, L., Quinones, R. A., Talaue-McManus, L.

(Eds.). Carbon and nutrient fluxes in continental margins. Springer, Berlin, pp.265-273 (2009).

44. Glenne, B., & Simensen, T. Tidal current choking in the landlocked fjord of Nordasvannet. *Sarsia* **11**, 43-73 (1963).

45. Schuller, S. E., Savage, C. Spatial distribution of diatom and pigment sedimentary records in surface sediments in Doubtful Sound, Fiordland, New Zealand. *New Zealand J. Marine Fresh. Res.* **45**, 591-608.

46. Faust, J. C., Knies, J., Slagstad, T., Vogt, C. & Milzer, G. Geochemical composition of Trondheimsfjord surface sediments: Sources and spatial variability of marine and terrigenous components. *Cont. Shelf Res.* **88**, 61-71.

47. R. H. Smittenberg *et al.* Pre- and post-industrial environmental changes as revealed by the biogeochemical sedimentary record of Drammensfjord, Norway. *Mar. Geol.* **214,** 177-200 (2005).

48. Huguet, C., Smittenberg, R. H., Boer, W., Sinninghe Damste, J. S. S. & Schouten, S. Twentieth century proxy records of temperature and soil organic matter input in the Drammensfjord, southern Norway. *Org. Geochem.* **38**, 1838-1849 (2007).

49. Smittenberg, R. H., Pancost, R. D., Hopmans, E. C., Paetzel, M., Sinninghe Damste, J. S. (2004) A 400-year record of environmental change in an euxinic fjord as revealed by the sedimentary biomarker record. Paleogeography, Palaeoclimatology, Palaeoecology 202, 331-351.

50. Skei, J. Geochemical and sedimentological considerations of a permanently anoxic fjord – Framvaren, South Norway. *Sed. Geol.* **36**, 131-145 (1983).

51. Velinsky, D. J. & Fogel, M. L. Cycling of dissolved and particulate nitrogen and carbon in the Framvaren Fjord, Norway: stable isotopic variations. *Marine Chem.* **67**, 161-180.

52. A. Muller. Geochemical expressions of anoxic conditions in Nordasvannet, a land-locked fjord in western Norway. *App. Geochem.* **16**, 363-374 (2001).

53. Nordberg, K., Filipsson, H. L., Gustafsson, M., Harland, R. & Roos, P. Climate, hydrographic variations and marine benthic hypoxia in Koljo Fjord, Sweden. *J. Sea Res.* **46**, 187-200 (2001).

54. Nordberg, K., Filipsson, H. L., Linne, P. & Gustafsson, M. Stable oxygen and carbon isotope information on the extablishment of a new, opportunistic foraminiferal fauna in a Swedish Skagerrak fjord basin, in 1979/1980. *Marine Micropaleontology* **73**, 117-128 (2009).

55. P. S. Loh, A. D. Reeves, S. M. Harvey, J. Overnell, A. E. J. Miller. The fate of terrestrial organic matter in two Scottish sea lochs. *Estuar. Coast. Shelf Sci.* **76**, 566-579 (2008).

56. Syvitski, J. P. M., Andrews, J. T. & Dowdeswell, J. A. Sediment deposition in an iceberg-dominated glacimarine environment, East Greenland: basin fill implications. *Global and Planet. Change* **12**, 251-270 (1996).

57. Smith, L. M. & Andrews, J. T. Sediment characteristics in iceberg dominated fjords, Kangerlussuaq region, East Greenland. *Sedimentary Geology* **130**, 11-25 (2000).

58. Smith, L. M., Alexander, C. & Jennings, A. E. Accumulation in East Greenland Fjords and on the continental shelves adjacent to the Denmark Strait over the Last Century based on 210Pb geochronology. *Arctic* **55**, 109 – 122 (2002).

59. Winkelmann, D., Knies, J. Recent distribution and accumulation of organic carbon on the continental margin west off Spitsbergen. *Geochem. Geophys. Geosys.* **6**, Q09012 (2005).

60. Wehrmann, L. M., Formolo, M. J., Owens, J. D., Raiswell, R., Ferdelman, T. G., Riedinger, N., Lyons, T. W. Iron and manganese speciation and cycling in glacially influenced high-latitude fjord sediments (West Spitsbergen, Svalbard): Evidence for a benthic recycling-transport mechanism. *Geochim. Cosmochim. Acta* (2014).

61. Louchouarn, P., Lucotte, M., Canuel, R., Gagne, J.-P. & Richard, L.-F. Sources and early diagenesis of lignin and bulk organic matter in the sediments of the Lower St. Lawrence Estuary and the Saguenay Fjord. *Mar. Chem.* **58**, 3-26 (1997).

62. Louchouarn, P., Lucotte, M. & Farella, N. Historical and geographical variations of sources and transport of terrigenous organic matter within a large-scale coastal environment. *Org. Geochem.* **30**, 675-699 (1999).

63. Tremblay, L. & Gagne, J.-P. Distribution and biogeochemistry of sedimentary humic substances in the St. Lawrence Estuary and the Saguenay Fjord, Quebec. *Org. Geochem.* **38**, 682-699 (2007).

64. Syvitski, J. P. M., LeBlanc, W. G. & Cranston, R. E. *The flux and preservation of organic carbon in Baffin Island fjords*. In: J.A. Dowdeswell and J.D. Scourse (eds.) Glaciomarine Environments: Processes and Sediments. Geological Society, London, Spec. Publ. 53: 217-239. 1990.

65. Walsh, E. M., Ingalls, A. E. & Keil, R. G. Sources and transport of terrestrial organic matter in Vancouver Island fjords and the Vancouver-Washington Margin: A multiproxy approach using d13Corg, lignin phenols, and the ether lipid BIT Index. *Limnol. Oceanogr.* **53**, 1054-1063 (2008)

66. Walinsky, S. E., et al. Distribution and composition of organic matter in surface sediments of coastal southeast Alaska. *Cont. Shelf. Res.* **29**, 1565-1579 (2009).

67. Silva, N. & Prego, R. Carbon and Nitrogen spatial segregation and stoichiometry in the surface sediments of Southern Chilean inlets (41-56S). *Estuarine, Coastal and Shelf Sci* **55**, 763-775 (2002).

68. N. Silva, C. A. Vargas, R. Prego. Land-ocean distribution of allochthonous organic matter in surface sediments of the Chiloe and Aysen interior seas (Chilean Northern Patagonia). *Continental Shelf Research* **31**, 330-339 (2011).

69. Lafon, A., Silva, N. & Vargas, C. A. Contribution of allochthonous organic carbon across the Serrano River Basin and the adjacent fjord system in Southern Chilean Patagonia: Insights from the combined use of stable isotope and fatty acid biomarkers. *Prog. Oceanogr.* (2014)

70. Mayr, C. et al. Responses of nitrogen and carbon deposition rates in Comau Fjord (42S, southern Chile) to natural and anthropogenic impacts during the last century. *Cont. Shelf Res.* **78**, 29-38 (2014).

71. Smith, R. W., Bianchi, T. S. & Savage, C. Comparison of lignin phenols and Doubtful Sound, Fiordland, New Zealand. *Org. Geochem*. **41**, 281-290 (2010).

72. Sinninghe Damste, J. S. S., Rijpstra, W. I. C., Coolen, M. J. L., Schouten, S. & Volkman, J. K. Rapid sulfurization of highly branched isoprenoid (HBI) alkenes in sulfidic Holocene sediments from Ellis Fjord, Antarctica. *Org. Geochem.* **38**, 128-139 (2007).

73. Yoon, H. I., Park, B.-K., Kim, Y. & Kim, D. Glaciomarine sedimentation and its paleoceanographic implications along the fjord margins in the South Shetland Islands, Antarctica during the last 6000 years. *Paleogeogr. Palaeoclimat. Palaeoeco.* **157,** 189-211 (2000).